Peptides 31 (2010) 412–418

Contents lists available at ScienceDirect

Peptides

journal homepage: www.elsevier.com/locate/peptides

The sea anemone *Bunodosoma caissarum* toxin BcIII modulates the sodium current kinetics of rat dorsal root ganglia neurons and is displaced in a voltage-dependent manner

Emilio Salceda [a,1], Omar López [a,1], André J. Zaharenko [b,c,*], Anoland Garateix [d], Enrique Soto [a]

[a] Instituto de Fisiología, Universidad Autónoma de Puebla, 14 sur 6301, CU, San Manuel, Puebla, Pue., CP 72750, Mexico
[b] Departamento de Fisiologia, Instituto de Biociências, Universidade de São Paulo, Rua do Matão, travessa 14, n: 321, CEP 05508-900, São Paulo, SP, Brazil
[c] Centro de Biotecnologia, Instituto de Pesquisas Energéticas e Nucleares (IPEN), Avenida Lineu Prestes, 2242, CEP 05508-000, São Paulo, SP, Brazil
[d] Centro de Bioproductos Marinos (CEBIMAR), Agencia de Medio Ambiente, Ministerio de Ciencia, Tecnología y Medio Ambiente (CITMA), Calle Loma entre 35 y 37, Alturas del Vedado, 10600, Ciudad de la Habana, Cuba

ARTICLE INFO

Article history:
Received 22 August 2009
Received in revised form 3 December 2009
Accepted 3 December 2009
Available online 16 December 2009

Keywords:
Site-3 toxins
Voltage-gated sodium channels
Fast inactivation
CgNa
ATX-II
Neurotoxins

ABSTRACT

Sea anemone toxins bind to site 3 of the sodium channels, which is partially formed by the extracellular linker connecting S3 and S4 segments of domain IV, slowing down the inactivation process. In this work we have characterized the actions of BcIII, a sea anemone polypeptide toxin isolated from *Bunodosoma caissarum*, on neuronal sodium currents using the patch clamp technique. Neurons of the dorsal root ganglia of Wistar rats (P5–9) in primary culture were used for this study (n = 65). The main effects of BcIII were a concentration-dependent increase in the sodium current inactivation time course (IC_{50} = 2.8 μM) as well as an increase in the current peak amplitude. BcIII did not modify the voltage at which 50% of the channels are activated or inactivated, nor the reversal potential of sodium current. BcIII shows a voltage-dependent action. A progressive acceleration of sodium current fast inactivation with longer conditioning pulses was observed, which was steeper as more depolarizing were the prepulses. The same was observed for other two anemone toxins (CgNa, from *Condylactis gigantea* and ATX-II, from *Anemonia viridis*). These results suggest that the binding affinity of sea anemone toxins may be reduced in a voltage-dependent manner, as has been described for α-scorpion toxins.

1. Introduction

Voltage-gated sodium channels (Na^+ channels) are integral membrane proteins which consist of an α-subunit (able to form functional ion channels when expressed in *Xenopus* oocytes) and two auxiliary subunits, β1 (or β3) and β2. The α-subunit has four homologous domains (I–IV) forming a ion pore; each domain has six transmembrane segments (S1–S6); the S4 transmembrane segments act as voltage sensors [6]. The intracellular loop between domains III and IV has been related with the fast inactivation gate, blocking the conduction pathway following channel activation [6].

A diversity of toxins and chemicals are known to either block or modulate Na^+ channels by binding to specific receptor sites. At least six neurotoxin receptor sites have been identified on the mammalian sodium channel [5,45]. Among them, receptor site 3 is a macrosite that involves the extracellular loops IS5–S6, IVS3–S4, and IVS5–S6 of the ionic channel with an important participation of the glutamic acid in position 1613 (rat brain Na^+ channel) [35] or the aspartic acid in position 1612 (rat cardiac Na^+ channel) [1].

The family of site-3 neurotoxins comprise a structurally diverse group of peptide toxins isolated from scorpions [4,25,33], sea anemones [28,30], spiders [18,24], and wasps [23,36]. These compounds increase the action potential duration by slowing down the time course of the sodium channel fast inactivation [32,37,40,41]. The binding affinity of site-3 toxins is decreased by depolarization [4,16], and several electrophysiological studies have shown that the dissociation rate of α-scorpion toxins is voltage-dependent [3,4,7,14,26,27,34,35,46,49]. A similar voltage-dependent dissociation for sea anemone toxins has been reported [49,46], however this has been a less explored characteristic of sea anemone toxins.

In this work we studied the electrophysiological effects of BcIII (from the sea anemone *Bunodosoma caissarum*), a sodium channel site-3 toxin, on macroscopic currents of rat dorsal root ganglia

* Corresponding author at: Departamento de Fisiologia, Instituto de Biociências, Universidade de São Paulo, Rua do Matão, travessa 14, n: 321, CEP 05508-900, São Paulo, SP, Brazil. Tel.: +55 11 30917522; fax: +55 11 30917568.
E-mail addresses: esalceda@siu.buap.mx (E. Salceda), omar.lpz.r@gmail.com (O. López), zaharenko@usp.br, a.j.zaharenko@ig.com.br (A.J. Zaharenko), cebimar@infomed.sld.cu (A. Garateix), esoto@siu.buap.mx (E. Soto).
[1] These authors contributed equally to this work..

0196-9781/$ – see front matter © 2009 Elsevier Inc. All rights reserved.
doi:10.1016/j.peptides.2009.12.005

(DRG) neurons. We found that under saturating concentration of the toxin, BcIII unbind from its receptor site in a voltage-dependent manner. Finally, we compare this latter result with those obtained in the presence of two other site-3 neurotoxins, CgNa (from *Condylactis gigantea*) and ATX-II (from *Anemonia sulcata*, now called *A. viridis*).

2. Materials and methods

2.1. Biological materials

Wistar rats at postnatal day 5–9 of either gender were used for the experiments. Animal care and procedures were in accordance with the National Institutes of Health Guide for the Care and Use of Laboratory Animals and the *Reglamento de la Ley General de Salud en Materia de Investigación para la Salud* of the *Secretaría de Salud* of Mexico. All efforts were made to minimize animal suffering and to reduce the number of animals used, as outlined in the "Guide to the Care and Use of Laboratory Animals" issued by the National Academy of Sciences.

2.2. Toxins

BcIII and CgNa were isolated and purified from the sea anemones *B. caissarum* and *C. gigantea* as previously described [31,44]. ATX-II was a gift from Professor L. Beress (Kiel, Germany). Aliquots of stock solution (200 μM) in deionized water were prepared and stored in a freezer (−20 °C). Before each experiment, an aliquot was dissolved in the perfusion solution.

2.3. Cell preparation

Young Wistar rats (P5–9) of either gender were anesthetized with ether and decapitated. DRG neurons were isolated and cultured according to the procedure described previously [37]. In order to guarantee the viability of the cells under study and to assure adequate spatial clamp, the neurons for recording were selected to have a rounded or oval shape, not to be adhered to other cells or to show any neurite outgrow, and to be refringent under the phase-contrast microscope.

2.4. Electrophysiological recording

A coverslip with attached neurons was transferred to a 500 μl perfusion chamber mounted on the stage of an inverted phase-contrast microscope (Nikon Diaphot, Tokyo, Japan). Cells were bathed with an external solution containing 20 mM NaCl, 1 mM $MgCl_2$, 1.8 mM $CaCl_2$, 45 mM TEA-Cl, 70 mM choline chloride, 10 mM 4-aminopyridine, and 5 mM HEPES (pH 7.4 adjusted with HCl). Osmolarity was monitored by a vapor pressure osmometer (Wescor, Logan, UT) and adjusted to 290 mOsm using dextrose.

A gravity-driven perfusion system maintained the external solution flowing into the chamber at a rate of about 100 μl/min. A pair of glass capillaries placed approximately 40 μm above the cell under study continuously microperfused (10 μl/min) external solution or external solution plus toxin.

Patch pipettes were pulled from borosilicate glass capillaries (TW120-3; WPI, Sarasota, FL), using a Flaming-Brown electrode puller (P80/PC; Sutter Instruments, San Rafael, CA). They typically had a resistance between 1 and 2.5 MΩ when filled with the internal solution which was composed as follows: 10 mM NaCl, 100 mM CsF, 30 mM CsCl, 10 mM TEA-Cl, 8 mM EGTA, and 5 mM HEPES (pH 7.2 adjusted with CsOH; osmolarity = 300 mOsm).

The whole-cell patch clamp technique was used to record ionic currents with an Axopatch-1D amplifier (Molecular Devices, Sunnyvale, CA). Command pulse generation and data sampling were controlled by the PClamp 8.0 software (Molecular Devices) using a 16-bit data acquisition system (Digidata 1320A, Molecular Devices). Signals were low-pass filtered at 5 kHz and digitized at 20 kHz. Leakage and capacitive currents were digitally subtracted using the P-P/n method; capacitance and series resistance (80%) were electronically compensated. In the time course of an experiment, seal and series resistance were continuously monitored to guarantee stable recording conditions. Experiments were made at room temperature (22–25 °C).

Experiments were rejected when, at the maximum peak current, the voltage error exceeded 5 mV after compensation of series resistance. No corrections were made for smaller values.

DRG neurons express a mixture of two sodium current (I_{Na}) subtypes: tetrodotoxin-sensitive (TTX-S; K_i = 0.3 nM) and tetrodotoxin-resistant (TTX-R; K_i = 100 μM). The type of I_{Na} in the cell under study was determined before each experiment and only those cells with <10% TTX-R I_{Na}, as derived from a steady-state inactivation profile, were used to determine the effects of BcIII on TTX-S I_{Na}.

It has been reported that both activation and steady-state inactivation curves are shifted over time in whole-cell patch clamp experiments [17,29]. In order to minimize the effects of time-dependent shifts on our results, recordings were not initiated until 10–15 min after the whole-cell configuration was obtained.

2.5. Data analysis

Recordings were analyzed off-line with PClamp 8.0 and Origin 8.0 (OriginLab Corporation, Northampton, MA) software. Statistical differences were determined using a Student's t test with a significance level of $P < 0.05$. Numerical data are presented as the mean ± SEM for at least four measurements, unless otherwise stated.

Concentration–response curve was obtained by measuring the time constant of the inactivation (τ_h) in sodium currents elicited by a single-step voltage protocol, where 40 ms depolarizing test pulses to −20 mV were applied from a holding potential (V_h) of −100 mV every 8 s. Data were then plotted as a function of toxin concentration and fit by the following function: $y = A_1 + (A_2 - A_1)/(1 + 10^{((\log IC50 - x) \times p)})$, where A_1 is the y value at the bottom plateau, A_2 is the y value at the top plateau, log IC_{50} is the x value when the response is halfway between A_1 and A_2, and p is the Hill slope.

Current–voltage relationships and availability curves were constructed using a standard double-pulse protocol in which, from a holding potential of −100 mV, a 40 ms test pulse to −20 mV was preceded by 40 ms prepulses between −120 and 70 mV at a stimulus rate of 0.125 Hz. The peak amplitudes of the currents were measured at the prepulse and converted to sodium chord conductance using the following equation: $G_{Na} = I_{Na}/(V_{test} - V_{rev})$, where G_{Na} is the sodium conductance, I_{Na} is the sodium current peak amplitude, V_{test} is the test potential and V_{rev} is the reversal potential for the sodium current.

The steady-state inactivation curve (h_∞) was calculated by dividing the current at a given prepulse by the maximum current achieved in the test pulse (I/I_{max}) and plotted as a function of the prepulse potential. Both steady-state activation and inactivation data were then fitted by a Boltzmann function.

To explore the state of the sodium channel on which BcIII exert their actions, two depolarizing trains of 200 pulses to −20 mV from a V_h of −100 mV (pulse duration of 40 ms, pulse interval of 200 ms) were applied. Between the first (control) and the second (test) trains there was a rest period of 1 min, during which the cell was held at a V_h of −100 mV and perfused with 10 μM BcIII.

Dissociation kinetics was measured with double-pulse protocols. From a V_h of −120 mV, a conditioning dissociation pulse to 0, +60 or +100 mV with increasing durations was applied, returning

to −120 mV for 20 ms. I_{Na} current was then elicited with a test pulse to −20 mV. In order to normalize the change in the maximum current amplitude and to quantify the degree of inactivation removal by the toxin, the ratio between the current at 5 ms after the start of the depolarization and the peak current ($I_{5\ ms}/I_{peak}$) was calculated. $I_{5\ ms}/I_{peak}$ gives an estimate of the probability for the channels not to be inactivated after 5 ms [14]: a zero value means full inactivation, a value of one means no inactivation. The average values of $I_{5\ ms}/I_{peak}$ from several experiments were plotted as a function of the conditioning pulse duration and fitted with a single-exponential function to obtain the dissociation time constants (τ_{off}).

3. Results

A total of 65 neurons were successfully patch-clamped for a sufficient time to allow the study of the action of BcIII. The capacitances of these cells formed a unimodal histogram with a mean of 53.6 ± 12.2 pF, which corresponds to a cell diameter of about 41 μm.

The change in peak amplitude, and the activation and inactivation time constants were calculated for I_{Na} before and about 2 min after toxin perfusion, time at which the maximum effect was reached. Concentration-response curve was built using 0.3, 1, 3 and 10 μM BcIII. For the rest of the experiments we used a 10 μM toxin concentration because it was the concentration at which the maximum effect was obtained.

The inactivation time course of the sodium current was well fitted by a single-exponential function (correlation coefficient ≥95%). Applying the single-step voltage protocol described in Section 2.5, the main effect of BcIII (10 μM) was a significant increase (n = 5; $P < 0.05$, Student's t test) on τ_h of 49.2 ± 7.3%; this effect was concentration-dependent with an IC_{50} = 2.8 ± 0.02 μM and a Hill slope coefficient of 0.76 ± 0.04 (n = 20) (Fig. 1). In addition, BcIII (10 μM) produced a significant increase (n = 5; $P < 0.05$, Student's t test) in the current amplitude of 41 ± 12%. The maximum effect of BcIII on τ_h occurred within the first 2 min after perfusion with toxin. Washout (5 min) removed 89 ± 3% of its effect (10 μM). The toxin did not affect the time course of I_{Na} activation.

Current density versus voltage curves were obtained from current–voltage relationships by normalizing ionic current amplitude as a function of membrane capacitance (Fig. 2). Under control conditions (n = 5), the maximum current density (−93.4 ± 15.9 pA/pF) was achieved at −20 mV. Perfusion with 10 μM BcIII significantly increased the maximum current density (−132.0 ± 15.8 pA/pF; n = 5; $P < 0.05$, Student's t test). The increase in the current density caused by BcIII was statistically significant in the voltage range between −20 and +10 mV. BcIII (10 μM) did not produce any significant change in the reversal potential of I_{Na}.

The sodium current chord conductance could be fitted by a Boltzmann function yielding half-maximal activation potential ($V_{1/2\ act}$) of −30.8 ± 0.9 mV under control conditions (n = 5), and −32.6 ± 1.6 mV in the presence of 10 μM BcIII (n = 5). The calculated slopes were 6.5 ± 0.4 and 5.3 ± 0.6 mV, respectively (Fig. 3A). These differences were not statistically significant ($P > 0.05$, Student's t test).

Steady-state inactivation profiles before and after BcIII (10 μM) were obtained with the double-pulse protocol detailed in Section 2.5. I/I_{max} versus voltage curves were fitted by a Boltzmann function. It was found that BcIII caused a nonsignificant hyperpolarizing shift in the half-maximal inactivation potential ($V_{1/2\ inact}$) from −60.1 ± 0.5 mV under control conditions (n = 5) to −64.8 ± 2.4 mV in the presence of the toxin (n = 5). The calculated slopes were 10.5 ± 0.5 and 12.7 ± 2.1 mV, respectively (Fig. 3B).

To explore the state of the sodium channel on which BcIII exerts its action, two voltage pulse trains separated by a rest period were applied (see Section 2.5). The inactivation time constant of the sodium current evoked by each pulse was plotted against the pulse number (Fig. 4). In control conditions τ_h remained relatively constant during the first 200 pulses. In contrast, τ_h of the ionic current produced by the first test pulse increased by 52.1 ± 11.6% following BcIII application, effect that was statistically significant (n = 3; $P < 0.05$, Student's t test). The effectiveness of BcIII did not increase by the remaining test pulses.

To investigate the possibility that BcIII (10 μM) may unbind from its receptor site in a voltage-dependent manner, a protocol of depolarizing prepulses with increasing durations was applied. The extent of fast inactivation removal was quantified by calculating the ratio $I_{5\ ms}/I_{peak}$. It was found that the rate of displacement was a function of the amplitude and duration of the prepulses, showing a progressive acceleration of fast inactivation with longer conditioning pulses (2.5–1000 ms) (Fig. 5). When prepulses to 0, +60 or

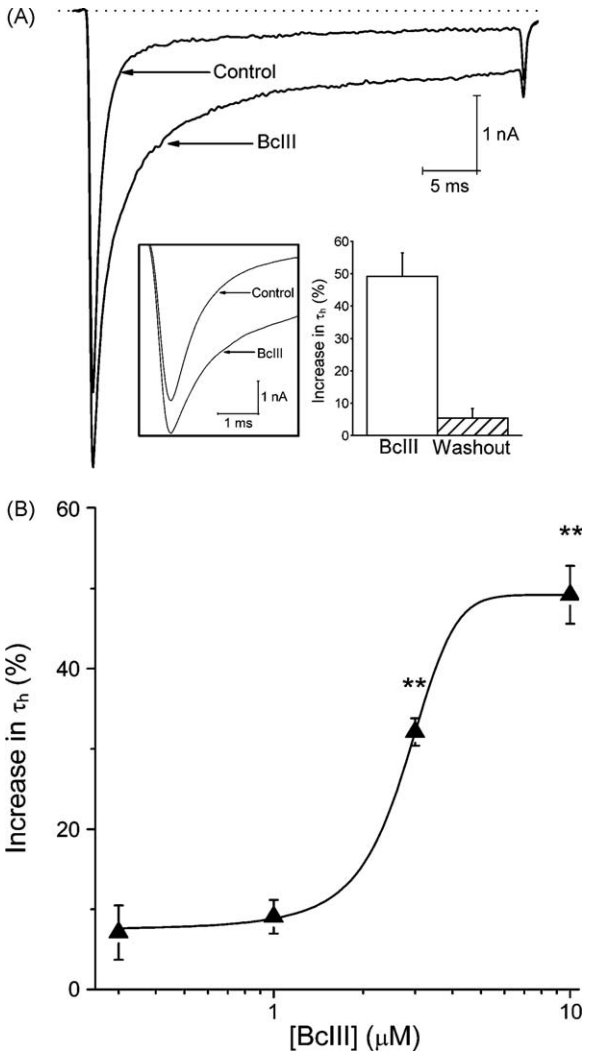

Fig. 1. BcIII increased the inactivation time course and the peak amplitude of sodium current. (A) Representative experiment showing the effects of 10 μM BcIII about 1 min after toxin perfusion. Currents were elicited by a single-step voltage protocol in which test pulses to −20 mV were applied from a V_h of −100 mV every 8 s In this and the following figures, the dotted line indicates the zero current level. Left inset is a zoom showing the increase in the current amplitude. Right inset shows the mean 10 μM BcIII effect on the inactivation time constant and its recuperation after toxin washout. (B) Concentration–response curve of the effect of BcIII (n = 20) on τ_h. Data were fitted (solid line) by a dose–response function yielding an IC_{50} of 2.8 ± 0.02 μM. In this and following graphs, the points represent the mean ± standard error of the mean and the asterisks denote significant effects with respect to control: $^{**}P < 0.01$, $^{*}P < 0.05$.

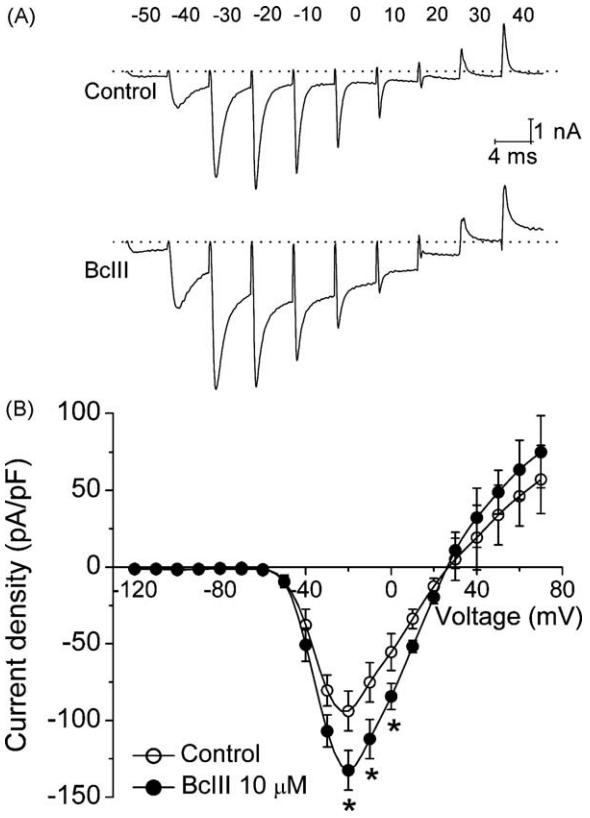

Fig. 2. Effects of BcIII on the current density versus voltage curve. (A) Sodium currents produced at different potentials (for clarity, only the first 4 ms of each record is presented) in the absence (top) and in the presence (bottom) of 10 μM BcIII. Currents were produced by 40 ms voltage pulses to the potentials indicated on top from a holding potential of −100 mV. BcIII affected the currents at all the shown voltages. (B) Current density versus voltage relationships ($n = 5$). Perfusion with 10 μM BcIII (closed circles) did not produce significant changes either on the voltage at which the maximum current density was reached or on the reversal potential.

+100 mV were applied, the values of τ_{off} were 285 ± 42, 164 ± 13, and 113 ± 8 ms, respectively ($n = 3$).

The kinetics of toxin dissociation has been studied for α-scorpion toxins, but it has been less explored for sea anemone toxins. Therefore, an interesting issue is to determine whether the effect of other site-3 anemone toxins may be decreased by depolarizing prepulses or, ultimately, whether they may be removed from its receptor site as consequence of strong depolarization. Thus, we decided to test whether the effects of two other known site-3 neurotoxins (CgNa, from *C. gigantea* and ATX-II, from *A. sulcata* (*A. viridis*)), at saturating concentrations, are decreased during depolarization. It was found that the values of τ_{off} were, for CgNa (10 μM, $n = 3$): 457 ± 55 and 265 ± 33 ms for conditioning prepulses of 0 and 60 mV, respectively; and for ATX-II (10 μM, $n = 3$): 347 ± 44 and 185 ± 20 ms (data not shown). Results show that these toxins also have a voltage-dependent dissociation kinetics.[2]

4. Discussion

In the present study the effects of the toxin BcIII, purified from the venom of the sea anemone *B. caissarum*, on the sodium currents in rat dorsal root ganglion cells were investigated using the whole-cell patch clamp technique. The main action of BcIII on these neurons was a slowing of the inactivation process of sodium current, with no significant effects on activation kinetics. Action of BcIII on I_{Na} was dependent on the concentration with an IC_{50} of 2.8 ± 0.02 μM. BcIII showed a voltage-dependent action on the slowing of the inactivation kinetics.

The increase in the inactivation time constant τ_h is the most notorious effect exerted by site-3 toxins [32,40,41]. The slowing of inactivation in the presence of BcIII is consistent with the idea that site-3 toxins destabilize the inactivated state of the sodium channels. The effect of BcIII in our experiments was almost totally removed by washout (5 min), in agreement with the data reported by other authors about the reversibility of the effects of sea anemone toxins upon vertebrate or insect Na^+ channels [2,9,40], in contrast with the irreversible toxicity on crustacean Na^+ channels [40].

Many gating models predict that the peak Na^+ current would be greater when inactivation is slowed or removed. Our results are in accordance with this prediction since BcIII increased the maximum Na^+ current amplitude at all test potentials. It has been demonstrated that scorpion α-toxins like Lqh-II, Lqh-III, and LqhαIT (purified from *Leiurus quinquestriatus hebraeus*) increased the peak Na^+ currents of the rat skeletal muscle sodium channels [14]. This effect could be a consequence of a prolonged open time of individual Na^+ channels. However, other site-3 toxins do not affect the peak sodium current or even decrease it. For example, many scorpion α-toxins only slightly increase or decrease the peak currents of Na^+ channels [19]. The same has been observed for ATX-II and LqTx (from the scorpion *L. quinquestriatus*) when applied on $Na_v1.2$ channels [35]. Similarly, the sea anemone toxins BgII, BgIII (both from *Bunodosoma granulifera*), ApC (from *Anthopleura elegantissima*) and CgNa (from *C. gigantea*) did not affect the current amplitude when applied to DRG neurons [37–39]. Therefore it is possible that some site-3 toxins may also produce some degree of channel blockade.

Perfusion with BcIII did not produce a significant change in the reversal potential, which indicates that the ion selectivity of Na^+ channels is not altered by this toxin. This is a marked difference with respect to the actions of site-2 toxins such as batrachotoxin, which also remove inactivation but significantly decrease the selectivity of the sodium channel [22,47].

In previous works [37–39] we have shown that other anemone toxins, when applied to DRG neurons, shifted the steady-state inactivation curve to hyperpolarizing values and caused a decrease in the voltage dependence of sodium channel inactivation by increasing the slope factor of the h_∞ curve. This latter effect has been also observed with site-3 toxins from scorpions [14], and wasps [36]. In the present work we have found that, in the presence of BcIII, there was a consistent tendency to shift to the left (i.e., to more hyperpolarized potentials) the voltage at which half of the channels are inactivated; however, this change was not statistically significant. The absence of effect on $V_{1/2\ inact}$ is not an exclusive property of BcIII: ATX-II does not induce a significant shift of the h_∞ curve when applied on hH1 (human heart subtype 1) or rSkM1 (rat skeletal muscle subtype 1) Na^+ channels [11]. Thus, some of the effects of site-3 toxins could be highly dependent on the sodium channel isoform and not on the characteristics of the toxins themselves. In fact, two previous studies about the actions of three anemone toxins (including BcIII) on different Na^+ channels subtypes (from $Na_v1.1$ to $Na_v1.7$) have shown differences in the manner in which each toxin affect the diverse isoforms of the voltage-gated sodium channel, including their actions on the steady-state voltage-dependent inactivation [31,48].

To explore the state of the sodium channel on which BcIII exert its effects, a post-resting voltage protocol was applied. In the presence of the toxin, the τ_h of the current elicited by the first pulse

[2] In our experimental conditions, the viability of the neurons was greatly reduced when long prepulses at +100 mV were applied. For this reason, and because our supply of toxins was limited, CgNa and ATX-II were not tested at this voltages.

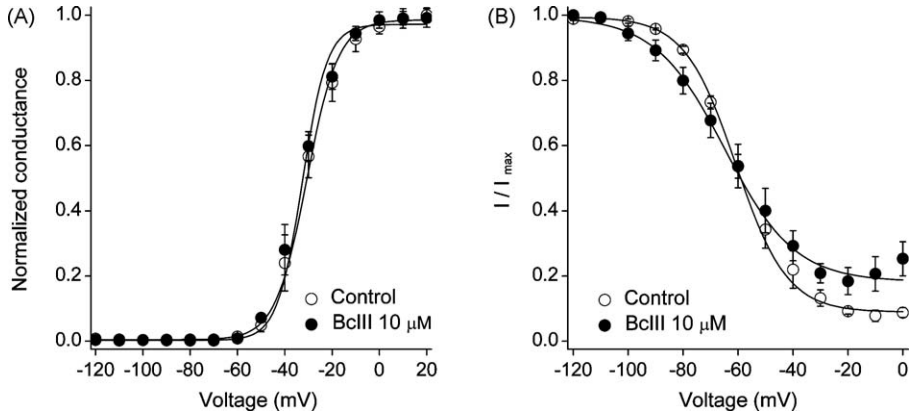

Fig. 3. Effects of BcIII on the voltage-dependence of I_{Na} conductance and steady-state inactivation. (A) G/G_{max} (normalized conductance) versus voltage curves before and after 10 μM BcIII. Continuous curves were obtained by fitting the data with a Boltzmann function yielding half-maximal activation of −30.8 ± 0.9 mV under control conditions (n = 5), and −32.6 ± 1.6 mV in the presence of 10 μM BcIII (n = 5). The calculated slopes were 6.5 ± 0.4 and 5.3 ± 0.6 mV, respectively. (B) Steady-state inactivation before and after 10 μM BcIII. The steady-state inactivation parameter (h_∞) was determined using the two-pulse protocol described in Section 2.5. BcIII caused a nonsignificant hyperpolarizing shift in the half-maximal inactivation potential from −60.1 ± 0.5 mV under control conditions (n = 5) to −64.8 ± 2.4 mV in the presence of the toxin (n = 5). The calculated slopes were 10.5 ± 0.5 and 12.7 ± 2.1 mV, respectively.

after a rest period increased as compared to the τ_h measured in the control train. This result indicate that BcIII has a high affinity for the closed state of the channel, as has been suggested for other site-3 toxins [13,14,39] and, accordingly, the toxin shows no preference for the sodium channel in the open state.

It has been reported that the binding affinity of site-3 toxins is decreased by depolarization [4,16], and a number of electrophysiological studies have shown that the rate at which α-scorpion toxins dissociate from its receptor site is voltage-dependent [3,4,7,14,26,27,34,35,46,49]. Only a few of these works have shown an analogous voltage-dependent dissociation for sea anemone toxins (generally for ATX-II, from *A. viridis* [46,49]), and since it has been proposed that nonidentical amino acids of the IVS3–S4 linker in the Na^+ channel participate in α-scorpion and sea anemone toxins binding to overlapping sites [35], a question to be answered is whether sea anemone toxins may also be removed from its receptor site as a consequence of depolarization. It was found that, with some quantitative differences probably attributable to the charge of the toxin molecules, the effect of BcIII, CgNa and ATX-II on τ_h was progressively decreased with longer conditioning pulses, and that the acceleration of fast inactivation was steeper as more depolarizing were the prepulses. As has been pointed elsewhere [13], several factors may affect the toxin affinity to voltage-gated Na^+ channels including the channel activation, fast and slow inactivation and membrane voltage. In our experiments BcIII did not affect the channel activation and hence there is only a small probability of a direct coupling between the toxin binding and the molecular substrate of Na^+ channel activation. Toxins could be removed by membrane voltage only by being in a position where they could sense the electrical field across the membrane, i.e., immersed into the membrane structure itself [3]; however, given the structural characteristics of site-3 toxins (a compact folding stabilized by three disulphide bridges, and patches of exposed negatively charged residues), this seems an unlikely explanation. Studies using liposomes containing phosphatidylserine and phosphatidylcholine showed that ApB toxin (from *Anthopleura xanthogrammica*) does not immerse into the membrane, contrary to the β-scorpion peptides, suggesting that the ApB interaction with sodium channel takes place in the extracellular region of the channel [43]. Most probably, structural torsions of the sodium channels upon strong depolarization may contribute to displace the peptides from their binding sites. Our experiments do not discard, however, the possibility of a toxin interaction with the slow inactivated state, but a direct experimental proof about this is difficult to achieve [13].

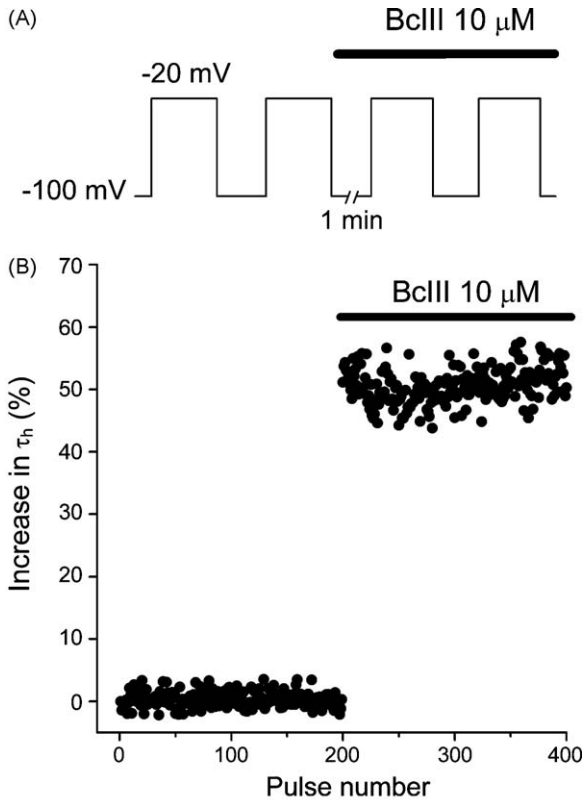

Fig. 4. BcIII acts on voltage-gated sodium channels in the closed state. (A) The toxin was applied at the beginning of the rest period (1 min) represented by the break. (B) Temporal course of the inactivation time constant τ_h in a typical experiment. The maximum effect of BcIII was already evident from the first pulse after the rest period. The bar indicates perfusion with 10 μM BcIII.

From the structural point of view, not only the positively charged amino acid residues (K/R35, K36) are important for binding of the sea anemone Type 1 toxins to sodium channels [21,31,35]. Comparing the primary sequence of CgNa, ATX-II and BcIII (Fig. 6), a negatively charged patch (D37 and E38) in CgNa do not affect the potency of this toxin, neither its mode of action on voltage-gated sodium channel. As a consequence, we may assume that the docking of each peptide to the channels should have the

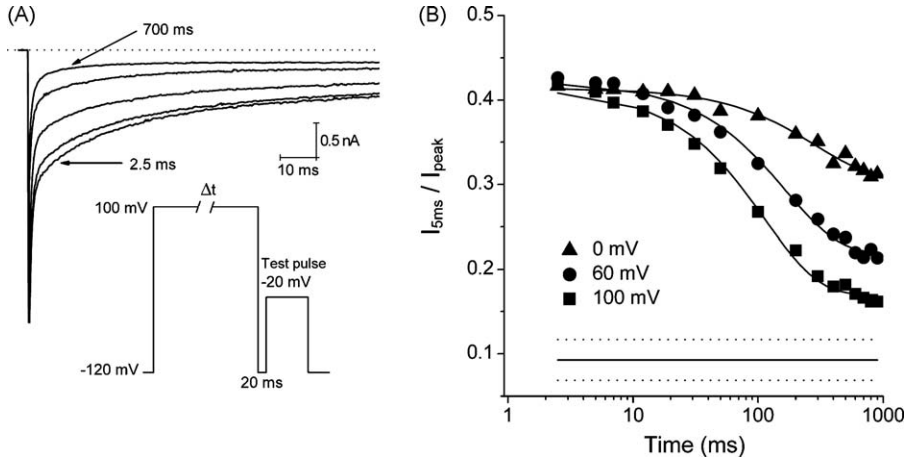

Fig. 5. The effect of BcIII is gradually removed by depolarization. (A) Superimposed current traces for a toxin-dissociation experiment in the presence of BcIII (10 μM). The inset shows the pulse protocol used. The superimposed traces show the progressive acceleration of inactivation caused by prepulses of different durations. For clarity, only five traces (2.5, 20, 50, 300 and 700 ms) are shown. Arrows show the currents obtained after conditioning pulses of 2.5 and 700 ms. (B) Dissociation curves obtained at the indicated prepulse voltages. Curves were fitted using a single-exponential function (continuous line) yielding the time constant, τ_{off}, for each conditioning voltage. The horizontal lines indicate the mean ± 1 SD in the absence of toxin.

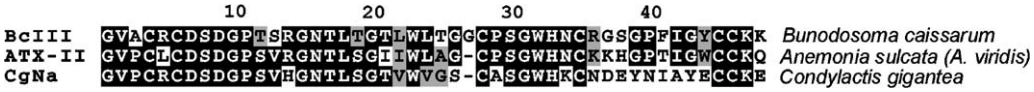

Fig. 6. Primary sequence alignment of the Type 1 sodium channel toxin BcIII (on top) with analogous peptide toxins ATX-II and CgNa. Black, gray and white backgrounds indicate identical, homologous and different amino acids, respectively. Cysteines are bonded as C1–C5, C2–C4 and C3–C6.

contribution of distinct amino acids in the contact surface. This aspect should be considered in more detail in future studies.

Further experiments are necessary to determine whether our observations have the same biophysical meaning that has been suggested for α-scorpion toxins by Campos et al. [3]. However, given that BcIII, CgNa and ATX-II modify the fast inactivation by binding to the closed state of Na^+ channels, and that site-3 toxin binding mainly occurs in the S3–S4 extracellular linker in domain IV of the Na^+ channel [35,8] and evidence associates the S4 segment in domain IV with the fast inactivation process [10,12,15,20,42], it is plausible that when depolarizing prepulses are applied, the electrical field on DIV-S4 reduces the binding strength of the receptor site.

Acknowledgments

Part of this work was supported by CONACyT (Consejo Nacional de Ciencia y Tecnología, México) grant I0110/127/08 and by the CNPq (Conselho Nacional de Desenvolvimento Científico e Tecnológico) grant 563874/2005-8.

References

[1] Benzinger GR, Kyle JW, Blumenthal M, Hanck DA. A specific interaction between the cardiac sodium channel and site-3 toxin Anthopleurin B. J Biol Chem 1998;273:80–4.
[2] Bosmans F, Aneiros A, Tytgat J. The sea anemone *Bunodosoma granulifera* contains surprisingly efficacious and potent insect-selective toxins. FEBS Lett 2002;532:131–4.
[3] Campos FV, Coronas FIV, Beirão PSL. Voltage-dependent displacement of the scorpion toxin Ts3 from sodium channels and its implication on the control of inactivation. Br J Pharm 2004;142:1115–22.
[4] Catterall WA. Membrane potential-dependent binding of scorpion toxin to the action potential Na^+ ionophore. Studies with a toxin derivative prepared by lactoperoxidase-catalyzed iodination. J Bio Chem 1977;252:8660–8.
[5] Catterall WA. Structure and function of voltage-gated ion channels. Annu Rev Biochem 1995;64:493–531.
[6] Catterall WA. From ionic currents to molecular mechanisms: the structure and function of voltage-gated sodium channels. Neuron 2000;26:13–25.
[7] Catterall WA, Ray R, Morrow CS. Membrane potential dependent binding of scorpion toxin to action potential Na^+ ionophore. Proc Natl Acad Sci USA 1976;73:2682–6.
[8] Cestèle S, Caterall WA. Molecular mechanisms of neurotoxin action on voltage-gated sodium channels. Biochimie 2000;82:883–92.
[9] Cestèle S, Kopeyan C, Oughideni R, Mansuelle P, Granier C, Rochat H. Biochemical and pharmacological characterization of a depressant insect toxin from the venom of the scorpion *Buthacus arenicola*. Eur J Biochem 1997;243:93–9.
[10] Chahine M, George Jr AL, Zhou M, Ji S, Sun W, Barchi RL, et al. Sodium channel mutations in paramyotonia congenita uncouple inactivation from activation. Neuron 1994;12:281–94.
[11] Chahine M, Plante E, Kallen RG. Sea anemone toxin (ATX II) modulation of heart and skeletal muscle sodium channel α-subunits expressed in tsA201 cells. J Membrane Biol 1996;152:39–48.
[12] Chanda B, Bezanilla F. Tracking voltage-dependent conformational changes in skeletal muscle sodium channel during activation. J Gen Physiol 2002;120:629–45.
[13] Chen H, Heinemann SH. Interaction of scorpion α-toxins with cardiac sodium channels: binding properties and enhancement of slow inactivation. J Gen Physiol 2001;117:505–18.
[14] Chen H, Gordon D, Heinemann SH. Modulation of cloned skeletal muscle sodium channels by the scorpion toxins Lqh II, Lqh III and LqhαIT. Pflügers Arch 2000;439:423–32.
[15] Chen LQ, Santarelli V, Horn R, Kallen RG. A unique role for the S4 segment of domain 4 in the inactivation of sodium channels. J Gen Physiol 1996;108:549–56.
[16] Couraud F, Rochat H, Lissitzky S. Binding of scorpion and sea anemone neurotoxins to a common site related to the action potential Na^+ ionophore in neuroblastoma cells. Biochem Biophys Res Commun 1978;83:1525–30.
[17] Fernandez JM, Fox AP, Krasne S. Membrane patches and whole-cell membranes: a comparison of electrical properties in rat clonal pituitary (GH3) cells. J Physiol 1984;356:565–85.
[18] Fletcher JI, Chapman BE, Mackay JP, Howden ME, King GF. The structure of versutoxin (δ-atracotoxin-Hv1) provides insights into the binding of site 3 neurotoxins to the voltage-gated sodium channel. Structure 1997;5:1525–35.
[19] Gordon D, Martin-Euclaire MF, Cestèle S, Kopeyan C, Carlier E, Khalifa RB, et al. Scorpion toxins affecting sodium current inactivation bind to distinct homologous receptor sites on rat brain and insect sodium channels. J Biol Chem 1996;271:8034–45.
[20] Horn R, Ding S, Gruber HJ. Immobilizing the moving parts of voltage-gated ion channels. J Gen Physiol 2000;116:461–76.
[21] Khera PK, Blumenthal KM. Importance of highly conserved anionic residues and electrostatic interactions in the activity and structure of the cardiotonic polypeptide anthopleurin B. Biochemistry 1996;35:3503–7.
[22] Khodorov BI. Chemicals as tools to study nerve fiber sodium channels: effect of batrachotoxin and some local anesthetics. Prog Biophys Mol Biol 1978;45:153–74.

[23] Kinoshita E, Maejima H, Yamaoka K, Konno K, Kawai N, Shimizu E, et al. Novel wasp toxin discriminates between neuronal and cardiac sodium channels. Mol Pharmacol 2001;59:1457–63.
[24] Little MJ, Zappia C, Gilles N, Connor M, Tyler MI, Martin-Eauclaire MF, et al. δ-Atracotoxins from Australian funnel-web spiders compete with scorpion α-toxin binding but differentially modulate alkaloid toxin activation of voltage-gated sodium channels. J Biol Chem 1998;273:27076–83.
[25] Meves H, Simard JM, Watt DD. Interactions of scorpion toxins with the sodium channel. Ann NY Acad Sci 1986;479:113–32.
[26] Mozhayeva GN, Naumov AP, Grishin EV, Soldatov NM. Effect of the toxins of the scorpion *Buthus eupeus* on the sodium channels of the membrane of the node of Ranvier. Biophysics 1979;4:242–9.
[27] Mozhayeva GN, Naumov AP, Nosyreva ED, Grishin EV. Potential-dependent interaction of toxin from venom of the scorpion *Buthus eupeus* with sodium channels in myelinated fibre: voltage clamp experiments. Biochim Biophys Acta 1980;597:587–602.
[28] Narahashi T, Moore JW, Shapiro BI. *Condylactis* toxin: interaction with nerve membrane ionic conductances. Science 1969;163:680–1.
[29] Nicholson GM, Willow M, Howden MEH, Narahashi T. Modification of sodium channel gating and kinetics by versutoxin from the Australian funnel-web spider *Hadronyche versuta*. Pflügers Arch 1994;428:400–9.
[30] Norton RS. Structure and structure–function relationships of sea anemone proteins that interact with the sodium channel. Toxicon 1991; 29:1051–84.
[31] Oliveira JS, Redaelli E, Zaharenko AJ, Cassulini RR, Konno K, Pimenta DC, et al. Binding specificity of sea anemone toxins to Na_v 1.1–1.6 sodium channels: unexpected contributions from differences in the IV/S3–S4 outer loop. J Biol Chem 2004;279:33323–35.
[32] Pelhate M, Hue B, Sattelle DB. Pharmacological properties of axonal sodium channels in the cockroach *Periplaneta americana* L. II. Slowing of sodium current turnoff by Condylactis toxin. J Exp Biol 1979;83:49–58.
[33] Possani LD, Becerril B, Delepierre M, Tytgat J. Scorpion toxins specific for Na^+ channels. Eur J Biochem 1999;264:287–300.
[34] Ray R, Catterall WA. Membrane potential dependent binding of scorpion toxin to the action potential sodium ionophore. Studies with a 3-(4-hydroxy 3-[^{125}I] iodophenyl) propionyl derivative. J Neurochem 1978; 31:397–407.
[35] Rogers JC, Qu Y, Tanada TN, Scheuer T, Catterall WA. Molecular determinants of high affinity binding of α-scorpion toxin and sea anemone toxin in the S3–S4 extracellular loop in domain IV of the Na^+ channel α subunit. J Biol Chem 1996;271:15950–62.
[36] Sahara Y, Gotoh M, Konno K, Miwa A, Tsubokawa H, Robinson HPC, et al. A new class of neurotoxin from wasp venom slows inactivation of sodium current. Eur J Neurosci 2000;12:1961–70.
[37] Salceda E, Garateix A, Soto E. The sea anemone toxins BgII and BgIII prolong the inactivation time course of the tetrodotoxin-sensitive sodium current in rat dorsal root ganglion neurons. J Pharmacol Exp Ther 2002;303:1067–74.
[38] Salceda E, Garateix A, Aneiros A, Salazar H, López O, Soto E. Effects of ApC, a sea anemone toxin, on sodium currents of mammalian neurons. Brain Res 2006;1110:136–43.
[39] Salceda E, Pérez-Castells J, López-Méndez B, Garateix A, Salazar H, López O, et al. CgNa, a type I toxin from the giant Caribbean sea anemone *Condylactis gigantea* shows structural similarities to both type I and II toxins, as well as distinctive structural and functional properties. Biochem J 2007;406:67–76.
[40] Salgado VL, Kem WR. Actions of three structurally distinct sea anemone toxins on crustacean and insect sodium channels. Toxicon 1992;30:1365–81.
[41] Shapiro BI, Lilleheil G. The action of anemone toxin on crustacean neurons. Comp Biochem Physiol 1969;28:1225–41.
[42] Sheets MF, Kyle JW, Kallen RG, Hanck DA. The Na^+ channel voltage sensor associated with inactivation is localized to the external charged residues of domain IV, S4. Biophys J 1999;77:747–57.
[43] Smith JJ, Alphy S, Seibert AL, Blumenthal KM. Differential phospholipid binding by site 3 and site 4 toxins. Implications for structural variability between voltage-sensitive sodium channel domains. J Biol Chem 2005;280:11127–33.
[44] Ständker L, Beress L, Garateix A, Christ T, Ravens U, Salceda E, et al. A new toxin from the sea anemone *Condylactis gigantea* with effect on sodium channel inactivation. Toxicon 2006;48:211–20.
[45] Strichartz G, Rando T, Wang GK. An integrated view of the molecular toxinology of sodium channel gating in excitable cells. Annu Rev Neurosci 1987;10: 237–67.
[46] Strichartz GR, Wang GK. Rapid voltage-dependent dissociation of scorpion α-toxins coupled to Na channel inactivation in amphibian myelinated nerves. J Gen Physiol 1986;88:413–35.
[47] Wang SY, Mitchell J, Tikhonov DB, Zhorov BS, Wang GK. How batrachotoxin modifies the sodium channel permeation pathway: computer modeling and site-directed mutagenesis. Mol Pharmacol 2006;69:788–95.
[48] Wanke E, Zaharenko AJ, Redaelli E, Schiavon E. Actions of sea anemone type 1 neurotoxins on voltage-gated sodium channel isoforms. Toxicon 2009;54: 1102–11.
[49] Warashina A, Fujita S, Satake M. Potential-dependent effects of sea anemone toxins and scorpion venom on crayfish giant axon. Pflügers Arch 1981;391: 273–6.